



Electronic signatures of topological disorder in amorphous graphene

Yuting Li^{1,2}, David A. Drabold^{1,2}

¹Department of Physics and Astronomy, Ohio University, Athens, OH 45701, USA

²Condensed Matter and Surface Science Program

E-mail: drabold@ohio.edu

Abstract: There have been extensive studies of the many phases of carbon, involving diamond and graphite, fullerenes, carbon nanotubes, amorphous carbon [1–3] and Schwarzites. In this study, the authors explore the impact of topological disorder (odd-membered rings) on the electron localisation of amorphous graphene. The authors employ realistic structural models, and find that the electronic states around Fermi level are highly localised around odd-membered rings. They predict an scanning tunnelling microscopic image for the amorphous surface. The authors' results also suggest that for two-dimensional system, there exist highly localised states well above the Fermi energy not at a band edge, which is rare in three-dimensional system. Phonon calculations reveal that certain atoms in the network are involved in both localised electronic and localised vibrational states, leading us to expect a large electron–phonon coupling between these, which might have interesting observable consequences.

1 Introduction

The remarkable discovery of Graphene has created a burgeoning scientific field replete with important and interesting questions, both basic and applied. In semiconducting crystals, it is well established that electronic applications depend critically upon impurities (dopants) added, and the character of defects and tail states, near the Fermi level. In fact, as a general rule, departures from ideal crystallinity are important for any electronic applications. In this context, it is natural to wonder about the consequences of defects in graphene. Soon after the discovery of the material, Castro Neto *et al.* [4] determined the electronic effects because of certain types of disorder. In this contribution, we explore the effects of topological disorder. In graphene, the mildest form of such disorder is odd-membered rings in the otherwise hexagonal net. If introduced into computer models with care, such rings can cost very-little energy and thus may be found in nature. Electron or ion beam damage is known to create such structures, and perhaps the first sighting of odd-membered rings was by Geim [5].

It is worth quickly contrasting the situation with amorphous Si. In the 1960s, there was great puzzlement over the existence of an optical gap arguably *larger* than in the diamond form. At the time, gaps were understood to be consequences of translational periodicity. In the end, it was found that an amorphous network maintaining tetrahedral order maintained an optical gap – the states near the Fermi level were not overly sensitive to the disorder of the a-Si network. Similar arguments can be made for other amorphous materials. Thus, it was a surprise that with an analogous form of topological disorder in grapheme, the

answer is completely different. That is, the semimetallic density of states (DOS) is strongly disrupted by odd-membered rings. As such, we can predict that odd-membered rings will profoundly affect charge carrier transport in amorphous graphene.

Spatially localised electronic states occur uniquely in solid state systems with disorder. Since the time of Anderson [6] in the 1950s, it was shown that in the presence of sufficient disorder, certain electron states decay exponentially in space. The study of localisation has become one of the most important aspects of condensed matter theory. Localisation in three-dimensional systems has been well studied [7–10]. The celebrated ‘Gang of Four’ paper discusses localisation from scaling theory, and compares one, two and three dimensions [11]. For the two-dimensional case, it has been shown theoretically and experimentally that localisation can be introduced by defects, as seen in the three-dimensional systems [12, 13]. In this paper, we will show that in amorphous graphene, the localised eigenstates emerge from odd-membered ring defects in an otherwise ideal sp^2 system, and we characterise this localisation with a realistic Hamiltonian.

Previous calculations reveal that the planar symmetry of amorphous graphene could be easily broken, because of the existence of odd-membered rings [14]. Here, we will show a few electronic states well above the Fermi level could be strongly coupled with several high-frequency phonon modes, which are also highly localised at odd-membered rings. This observation is perhaps reminiscent the polaron study in thin films of liquid He, where Jackson and Platzman showed the motion of a single electron in the plane is highly coupled with the thermally excited ripples in two-dimensional surface [15].

Table 1 Ring statistics of 200 a-g model, shown as %

ring size	5	6	7
percentage	38.5	53.9	7.7

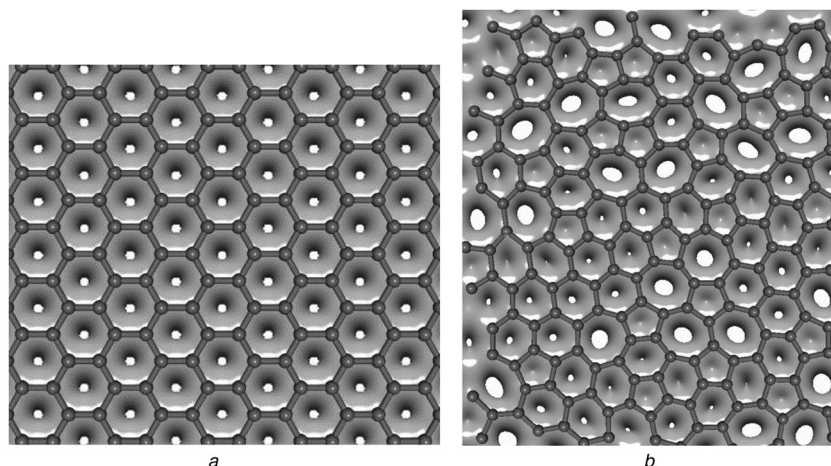
2 Model

To evaluate the charge density and spatial localisation, a 200-atom amorphous graphene model (200 a-g), prepared by a Wooten–Weaire–Winer annealing scheme [16], is employed. This model has ideal 3-fold coordination, and ring statistics are given in

Table 1: This 200 a-g model is a realisation of the continuous random network (CRN) concept proposed by Zachariassen [17]. The CRN idea reflects the notion that the *local* structure and bonding topology should be as much like the crystal as possible, while allowing minor variations in bond angle and bond lengths to ensure that the energy is close to the crystalline phase. A 288-atom crystalline graphene model (288 c-g) was also used to compare the results with amorphous graphene models.

3 Charge density

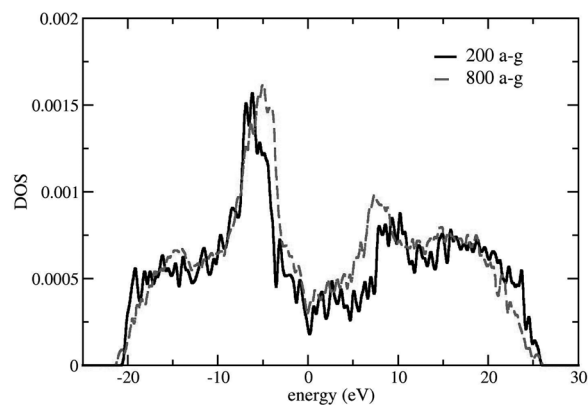
To study amorphous graphene, we employ an *ab initio* program SIESTA [18, 19], using pseudopotentials and the Perdew–Zunger parameterisation of local-density approximation. In both crystalline and amorphous cases, the minimal basis set (single- ζ basis) and self-consistency were applied. The simulated scanning tunnelling microscope images according to charge density calculation results are shown in Fig. 1. For crystalline graphene, the electrons in p orbitals are delocalised on the graphene sheet giving rise to aromaticity. Then the charges are expected to distribute uniformly on the honeycomb lattice of graphene, as shown in Fig. 1a. By contrast, the existence of odd-membered rings disturbs this uniformity, introducing several holes associated with seven-membered rings, and charge is notably localised at five-membered rings. These calculations are in close agreement with published density functional theory (DFT) calculation results of pure crystalline graphene [20] and crystalline graphene with defects [21].

**Fig. 1** Simulated scanning tunneling microscope images (total charge density) for both crystalline and amorphous graphene models

Atom configurations are represented by grey balls and sticks

a Charge density of 288 c-g model

b Charge density of 200 a-g model

**Fig. 2** DOS of 200-atom a-g and 800-atom a-g models [14]

Solid line represents the DOS of 200 a-g, with the DOS of 800 a-g is given by dashed line. The Fermi level is at 0 eV

4 Density of states

The Γ -point DOS of planar 200 a-g model was calculated using the same computational approach as charge density. As we shown in Ref. [14], in an 800 atom amorphous graphene model, the odd-membered rings generate a number of states around the Fermi level. The DOS of 200 a-g model is very similar to the 800 a-g model, as shown in Fig. 2. We conclude that odd-membered rings always have a significant impact on the DOS near the Fermi level. A logical extension of our work would be to discover quantitatively how the DOS near the Fermi level evolves as a function of ring concentration.

5 Localised states

As we previously pointed out, the planar symmetry of amorphous graphene is unstable with respect to tiny external out-of-plane distortions, giving rise to pentagonal puckering and lowering the total energy [14, 22]. In the following, localisation properties of eigenstates for both planar and puckered models are explored. To characterise the spatial localisation of electronic states, inverse

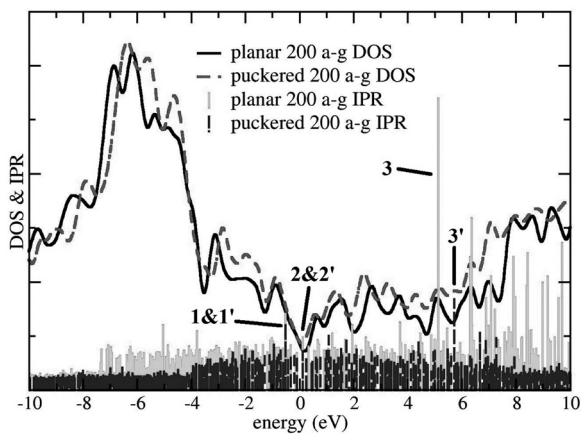


Fig. 3 Scaled DOS and inverse participation ratio of planar and puckered 200 a-g models. The Fermi level is at 0 eV

participation ratio (IPR) calculations were performed. The IPR is defined as [23]: $I(\psi_j) = N \sum_{i=1}^N a_i^4 / (\sum_{i=1}^N a_i^2)^2$,

where $\psi_j = \sum_{i=1}^N a_i^j \phi_i$ is the j th eigenvector. The results are depicted in Fig. 3. Around the Fermi level (0 eV), there are two localised states in planar 200 a-g model, marked as peak 1 and peak 2 in Fig. 3, and the most localised state is found around 5 eV, marked as peak 3. Correspondingly, the eigenstates are named state 1, state 2 and state 3. Similar calculations have also been performed for a puckered 200 a-g model. Similarly, the IPR calculation shows two localised eigenstates around Fermi level (0 eV), marked as peak 1' and 2' in Fig. 3. And the most localised peak is also found around 5 eV, marked as peak 3' in Fig. 3. These peaks are named as state 1', state 2' and state 3' respectively.

To visualise the spatial structure of these localised states, the charge density of each conjugate eigenstate is plotted, as shown in Figs. 4 and 5. For the planar 200 a-g model, peak 1 is found around the valence tail, and localised around an area with a higher percentage of pentagons, as shown in Fig. 4a. In contrast, for the conduction edge, peak 2 is distributed around an area with higher percentage of heptagons, as shown in Fig. 4b. For the puckered 200 a-g model, the energy levels of peak 1' and 2' are close to peak

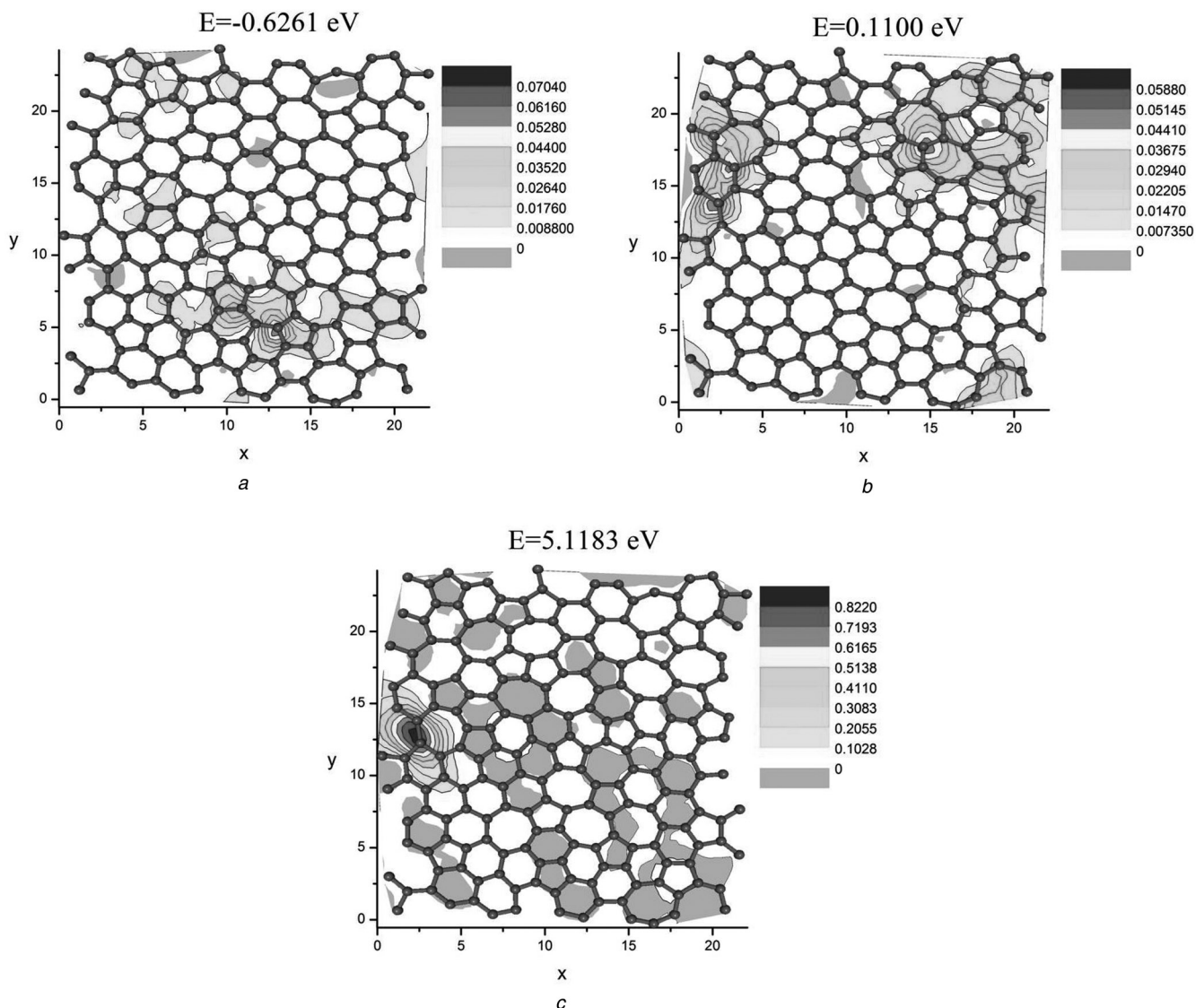


Fig. 4 Three localised eigenstates of planar 200 a-g model, depicted as peak 1–3 in Fig. 3. Here $E_f = 0$ eV. Axes are in units of Å

a Eigenstate for peak 1 in Fig. 3

b Eigenstate for peak 2 in Fig. 3

c Eigenstate for peak 3 in Fig. 3

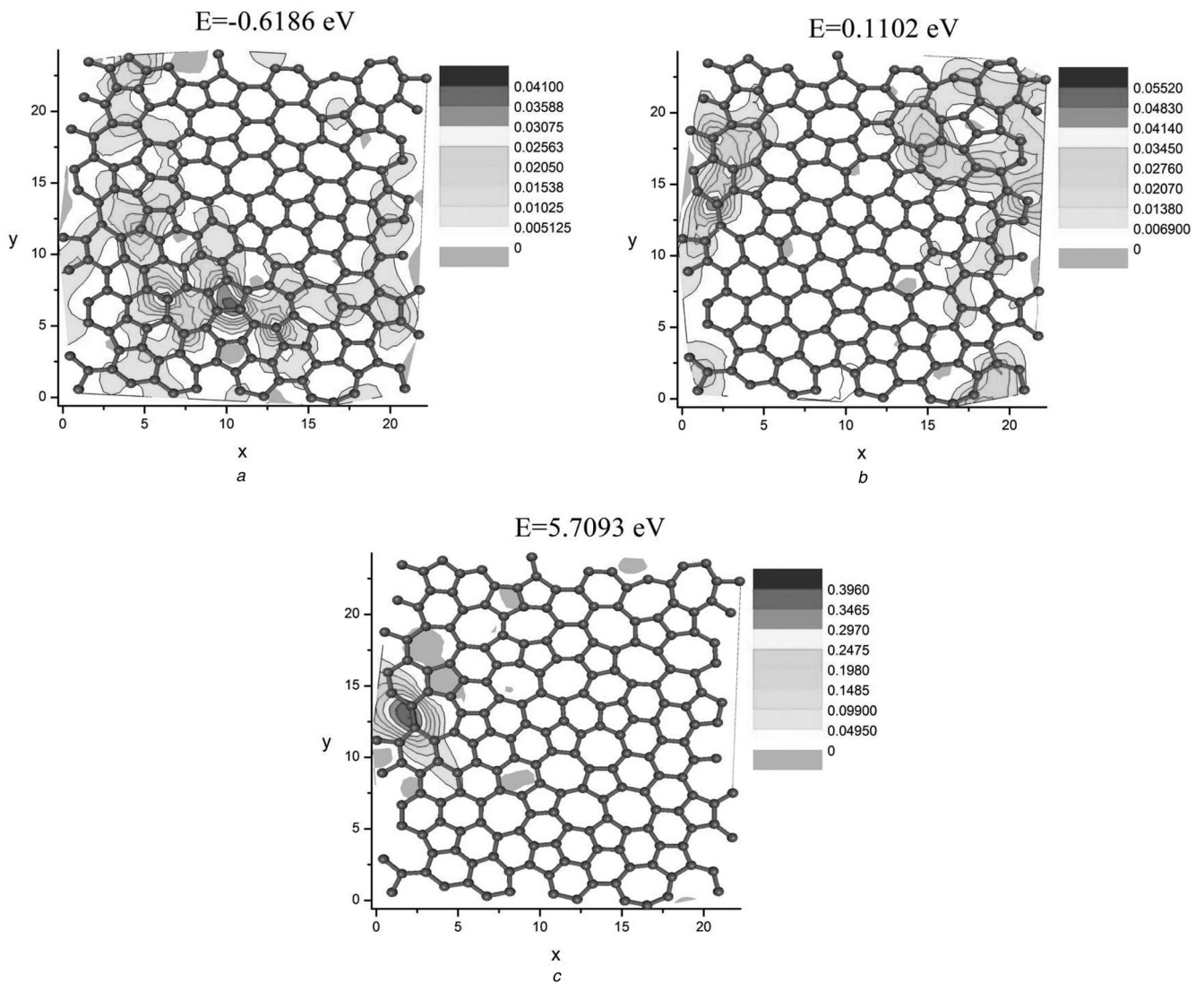


Fig. 5 Three localised eigenstates of puckered 200 a-g model, depicted as peak 1'-3' in Fig. 3. $E_f = 0$ eV. Axes are in units of Å
 a Eigenstate for peak 1' in Fig. 3
 b Eigenstate for peak 2' in Fig. 3
 c Eigenstate for peak 3' in Fig. 3

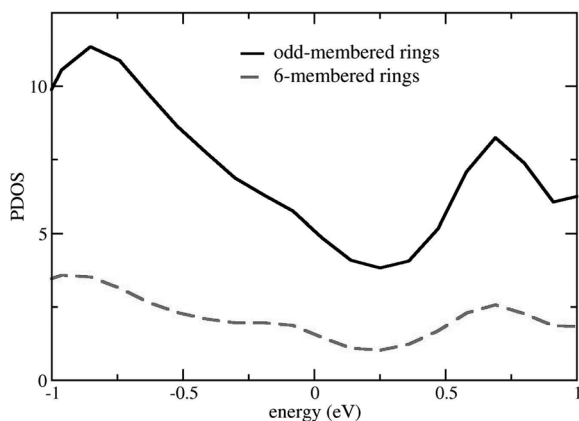


Fig. 6 Projected DOS of planar 200 a-g model. Fermi level is at 0 eV

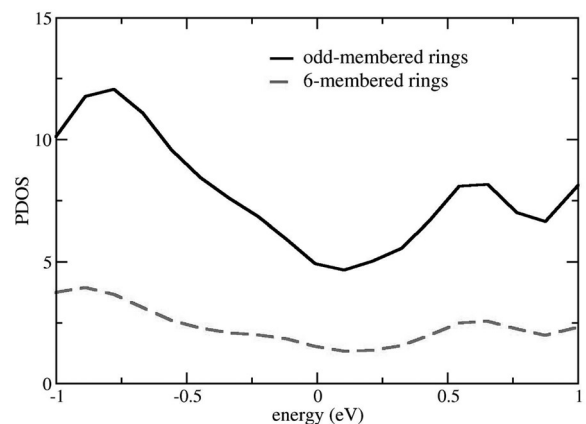


Fig. 7 Projected density of states of puckered (relaxed) 200 a-g model. Fermi level is at 0 eV

1 and 2. As shown in Fig. 5a, at valence edge, state 1' and state 1 are distributed over a similar high-pentagon-ratio area. And at the conduction edge, state 2' is localised

around an area with high heptagon-ratio, as shown in Fig. 5b, analogous to state 2. Thus the presence of odd-membered rings in amorphous graphene gives rise to

various eigenstates around the Fermi level, leading to vast difference in DOS between crystalline and amorphous graphene [14, 24].

Next, we explored the electronic consequences of puckering, induced by pentagonal structures. We employ the projected DOS (PDOS) computed for both planar and puckered 200 a-g models, using SIESTA with SZ basis, as shown in Figs. 6 and 7. Near the Fermi level, the contributions because of pentagons and heptagons are higher than hexagons, which is consistent with our observation from the localised eigenstates: the localisation around Fermi level is associated with odd-membered rings. However, most atoms in odd-membered rings are shared between pentagonal and heptagonal rings. Then at valence edge or conduction edge, on the basis of PDOS calculation, it is hard to distinguish whether the localisation around the Fermi level originates from pentagons or heptagons.

The most localised state in planar 200 a-g model is state 3. Its energy level is around 5 eV in the conduction band, and state 3 is highly localised on two atoms shared by two heptagons, as shown in Fig. 4c. In the puckered case, state 3' is found at the exact same position at state 3, given in Fig. 5c. This is similar to the situation observed in glassy GeSe₂ model by Zhang and Drabold [8]. They found that the most defective sites lead to certain localised states far inside the valence and conduction bands.

As illustrated in Fig. 3, the global localisation degree of puckered 200 a-g model is lower than the planar 200 a-g model. Around the Fermi level, puckered models illustrate localised eigenstates with relatively lower localisation degree comparing with the planar model. The reduction in strain from puckering helps to delocalise the electronic states. Whereas, in the valence and conduction bands, the localisation degree of eigenstates in puckered amorphous graphene model is significantly decreased compared with planar model. Taking state 3 and 3' as example, even though they are localised on the same atoms, state 3' possesses higher energy level and significantly lower localisation degree, as shown in Fig. 3.

Where electronic applications are concerned, this paper establishes that the DOS is sensitive to odd-membered rings. From the Kubo–Greenwood formula, one can express conductivity in the DC-limit as [25]

$$\sigma(T) = -\frac{1}{3} \sum_{\alpha} \int_{-\infty}^{\infty} \sigma_{\alpha\alpha}(\varepsilon) \frac{\partial f_F(\varepsilon)}{\partial \varepsilon} d\varepsilon \quad (1)$$

where the diagonal elements of the conductivity tensor are

$$\sigma_{\alpha\alpha}(\varepsilon) = \frac{\pi e^2 \hbar}{\Omega m^2} \sum_{nm} |\langle \psi_n | p_{\alpha} | \psi_m \rangle|^2 \delta(\varepsilon_n - \varepsilon) \delta(\varepsilon_m - \varepsilon) \quad (2)$$

In this expression, $\alpha = x, y, z$, f_F is the Fermi distribution, e and m are the electronic charge and mass, p_x is the momentum operator, ψ_i and ε_i are the eigenstates and eigenvalues; Ω the cell volume. From (1), (2), the DC conductivity will involve transitions very near the Fermi level, precisely those states so strongly influenced by topological disorder. We have not yet evaluated this expression, but there is every reason to expect that a significant amount of ring disorder will destroy the unique electronic properties of crystalline graphene.

6 Classical normal modes

Phonon calculations were performed for both planar and puckered 200 a-g models. Their dynamical matrixes were constructed, by computing forces on all atoms from six orthogonal displacements of 0.04 Bohr. In the high-frequency range, we found that several phonon modes are localised at the same range as state 3 and 3' in planar and puckered 200 a-g models respectively, as given in Figs. 4c and 5c. Two examples of planar and puckered 200 a-g modes are shown in Fig. 8.

These simulations reveal another interesting feature that merits further study. Inspection of Figs 4 and 5 (showing electron eigenstates) and Fig. 8 (showing vibrational modes on the same network) reveal that there are cases in which *the same* atoms participate in *both*—localised electron and vibrational modes. This is interesting, because one would expect an enormous electron–phonon coupling for such a case [10]. Thus, if the system could be locally probed at these joint ‘hot spots’ with electrons (phonons) a large response would be expected in the phonons (electrons). Figs. 8a, b and 4c show such a structure. We have not

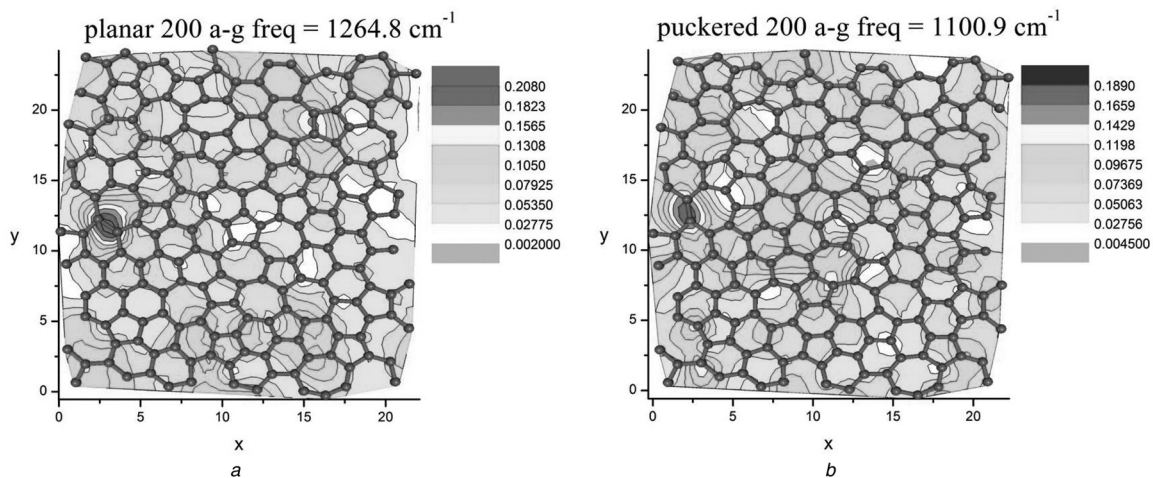


Fig. 8 Two localised high-frequency phonon modes in planar and puckered 200 a-g modes. Axes are in units of Å

a Localised high-frequency phonon mode in planar 200 a-g model

b Localised high-frequency phonon mode in puckered 200 a-g model

encountered this interesting spatial juxtaposition of localisation in our work on other amorphous materials. If an experiment could be formulated that probed the system at such points (or excited the localised vibrational mode), the electronic response might be substantial.

Finally, compared with the planar 200 a-g model, the intensity of these phonon modes are reduced in the puckered a-g model, as illustrated in Fig. 8.

7 Conclusion

In conclusion, we found that localised eigenstates in both planar and puckered amorphous graphenes originate from odd-membered rings. Around Fermi level, localised states at valence edge are found in the high-pentagon-ratio area. And the localised states at conduction edge are distributed in the area associated with more heptagons. Far inside the conduction edge, the most localised states in both planar and puckered amorphous graphene models are distributed on the same atoms associated with the junction of heptagons, and are strongly coupled with high-frequency phonon modes. The transport properties of amorphous graphene would be profoundly impacted by these localised states as seen from the Kubo–Greenwood formula (2) [25].

Also, the IPR calculations reveal that the localisation is higher in planar amorphous graphene model compared with the puckered configuration. This could be because of the reduction in strain by pentagonal puckering.

8 Acknowledgments

Here we want to acknowledge Dr. M. F. Thorpe and his group at Arizona State University. This work was supported by the Army Research Office.

9 References

- 1 Drabold, D.A., Stumm, P., Fedders, P.A.: 'Theory of diamond like amorphous carbon', *Phys. Rev. B*, 1994, **49**, pp. 16415
- 2 Drabold, D.A., Fedders, P.A., Grumbach, M.P.: 'Gap formation and defect states in tetrahedral amorphous carbon', *Phys. Rev. B*, 1996, **53**, pp. 5480
- 3 Dong, J., Drabold, D.A.: 'Ring formation and the structural and electronic properties of tetrahedral amorphous carbon surfaces', *Phys. Rev. B*, 1998, **57**, pp. 15591
- 4 Castro Neto, A.H., Guinea, F., Peres, N.M.R., Novoselov, K.S., Geim, A.K.: 'The electronic properties of grapheme', *Rev. Mod. Phys.*, 2009, **81**, pp. 109
- 5 Geim, A.K.: 'Graphene: status and prospects', *Science*, 2009, **324**, pp. 1530
- 6 Anderson, P.W.: 'Absence of diffusion in certain random lattices', *Phys. Rev.*, 1958, **109**, pp. 1492
- 7 Ludlam, J.J., Taraskin, S.N., Elliott, S.R., Drabold, D.A.: 'Universal features of localized eigenstates in disordered systems', *J. Phys.: Condens. Matter*, 2005, **17**, pp. L321–L327
- 8 Zhang, X., Drabold, D.A.: 'Structural and electronic properties of glassy GeSe₂ surfaces', *Phys. Rev. B*, 2000, **62**, pp. 15695
- 9 Dong, J., Drabold, D.A.: 'Atomistic structure of band-tail states in amorphous silicon', *Phys. Rev. Lett.*, 1998, **80**, pp. 1928
- 10 Atta-Fynn, R., Biswas, P., Drabold, D.A.: 'Electron-phonon coupling is large for localized states', *Phys. Rev. B*, 2004, **69**, pp. 245204
- 11 Abrahams, E., Anderson, P.W., Licciardello, D.C., Ramakrishnan, T.V.: 'Scaling theory of localization: absence of quantum diffusion in two dimensions', *Phys. Rev. Lett.*, 1979, **42**, pp. 673
- 12 Peres, N.M.R., Guinea, F., Castro Neto, A.H.: 'Electronic properties of disordered two-dimensional carbon', *Phys. Rev. B*, 2006, **73**, pp. 125411
- 13 Painter, O., Lee, R.K., Scherer, A., *et al.*: 'Two-dimensional photonic band-gap defect mode laser', *Science*, 1999, **284**, pp. 1819
- 14 Li, Y., Inam, F., Kumar, A., Thorpe, M.F., Drabold, D.A.: 'Pentagonal puckering in a sheet of amorphous Graphene', *Phys. Status Solidi B*, 2011, **248**, pp. 2082–2086
- 15 Jackson, S.A., Platzman, P.M.: 'Polaronic aspects of two-dimensional electrons on films of liquid He', *Phys. Rev. B*, 1981, **24**, pp. 499
- 16 Wooten, F., Winer, K., Weaire, D.: 'Computer generation of structural models of amorphous Si and Ge', *Phys. Rev. Lett.*, 1985, **54**, pp. 1392–1395
- 17 Zachariasen, W.H.: 'The atomic arrangement in Glass', *J. Am. Chem. Soc.*, 1932, **54**, pp. 3841–3851
- 18 Artacho, E., Ordejon, P., Soler, J., *et al.*: 'The SIESTA method; developments and applicability', *J. Phys.: Condens. Matter*, 2008, **20**, pp. 064208
- 19 Drabold, D.A., Sankey, O.F., Wang, R., Klemm, S.: 'Efficient ab initio molecular dynamics simulations of carbon', *Phys. Rev. B*, 1991, **43**, pp. 5132
- 20 Xu, P., Yang, Y., Barber, S.D., *et al.*: 'Giant surface charge density of graphene resolved from scanning tunneling microscopy and first-principles theory', *Phys. Rev. B*, 2011, **84**, pp. 161409o(R)
- 21 Warner, J.H., Lee, G.-D., He, K., Robertson, A.W., Yoon, E., Kirkland, A.I.: 'Bond length and charge density variations within extended arm chair defects in Graphene', *ACS Nano*, 2013, **7**, pp. 9860–9866
- 22 Li, Y., Drabold, D.A.: 'Symmetry breaking and low energy conformational fluctuations in amorphous grapheme', *Phys. Status Solidi B*, 2013, **250**, pp. 1012
- 23 Ziman, J.: 'Models of disorder, the theoretical physics of homogeneously disordered systems' (Cambridge University Press, 1979)
- 24 Kapko, V., Drabold, D.A., Thorpe, M.F.: 'Electronic structure of a realistic model of amorphous graphene', *Phys. Status Solidi B*, 2010, **247**, pp. 1197–1200
- 25 Abtew, T.A., Zhang, M., Drabold, D.A.: 'Ab initio estimate of the temperature dependence of electrical conductivity in a model disordered material: a-Si:H', *Phys. Rev. B*, 2007, **76**, pp. 045212